Journal of Neuroscience Methods, 38 (1991) 247–257

NSM 01258

An analysis of the oscillatory patterns in the central nervous system with the wavelet method

A.W. Przybyszewski

Department of Physiology, Freie Universität Berlin, Arnimallee 22, 1000 Berlin 33 (Germany)

(Received 21 September 1990)
(Revised version received 14 February and 12 April 1991)
(Accepted 12 April 1991)

Key words: Wavelet; Transient oscillation; Retina; Ganglion cell; Power spectrum; Time shift; Time dilation

This paper discusses a simple application of the wavelet transformation to analyse nerve cell impulse patterns. The action potentials converted into delta, or Dirac, functions were convoluted in the time domain with a modified Gauss (the negative of the second derivative of Gauss) function, varying in width between 0.6 and 384 ms. The width of the Gauss function was varied in 640 steps. Some parts of the transformation were extended, analysed and averaged in the frequency domain to explore oscillatory components of the impulse pattern. The sequences of action potentials of retinal ganglion cells evoked by short flashes are taken as examples. The present analysis demonstrate some properties of mathematical "microscopic" application to transient responses of the central nervous system (CNS), whereby the degree of magnification (steps of transformation) was varied.

Introduction

Responses of the CNS to complex as well as very simple stimuli have, as a rule, consisted of complicated response patterns when the sequence of action potentials was analysed in the time domain. Spontaneous activity complicates further the analysis of these responses. One of the most popular methods for analysing single neuron data in electrophysiology is the computation of PSTHs (post- or peri-stimulus time histograms).

A PSTH represents the average rat of action potentials discharged by a single nerve cell, whereby averaging is performed in equidistant time bins. The choice of bin width, which acts as a low-pass filter, is, of course, crucial. The larger the bin width, the lower the cut-off frequency of the filter. Conversely, when the bin width is very small compared with the average impulse interval of the discharging nerve cell, there is a high variability in the PSTH which necessitates an increase in the number of responses averaged.

To circumvent these difficulties it seems feasible to transform the spontaneous impulse rate into an analogue signal which can be analysed by standard techniques, e.g. computing fast Fourier transformations (FFT). These may lead to erroneous results (Schild and Schultens, 1986). French and Holden (1971) proposed a convolution of the impulse train with an appropriately selected function such as $\sin(x)/x$. After this transformation, an appropriate window must be selected (Harris, 1978) to avoid interference caused by the length of the recording. The sampling technique and FFT analysis can be applied to the responses following each stimulus; the power spectra of the

Correspondence: Dr. A.W. Przybyszewski, Department of Physiology, Freie Universität Berlin, Arnimallee 22, 1000 Berlin 33 (Germany). Tel.: (30) 8382551; Fax: (30) 8382507.

individual responses can then be averaged (O'Regan and Przybyszewski, 1987). Using this method, even averaged power spectra mask the transient oscillations because the oscillations represent only a small part of the total signal in the time domain. Therefore, it is meaningful to search for a method of analysis by which the "local" character of different frequency components is preserved.

Gabor (1946) was the first to use a sliding time gaussian window which is fixed in length when applying Fourier analysis to radar (narrow-band) signals. His goal was to detect certain frequency components in the analysed signal which only appeared locally in time. A disadvantage in applying this method to nerve cell signals is that it is a fixed window function in length. It is necessary, therefore, to select a function by which the sequence of action potentials, which are considered as Dirac functions, is appropriately convoluted; in analysing neurobiological responses, the convoluting function should be easily adaptable to the neurophysiological question. The wavelet transformation method fulfills the criteria for such a procedure.

Our objective was to find out whether using wavelet transformation is a more reliable method for determining the significance of different transient oscillations than the PSTH or FFT analysis as proposed by French and Holden (1971).

Methods

Combes, Grossman and Tchamitchian (1989) summarized the application of wavelet transformation for the analysis of transient signals. This procedure allows an analysis which may be local in both the frequency and the time domain. To reach this goal, the wavelet function

$$g_{a,b}(t) = a^{-1/2} g\left(\frac{t-b}{a}\right) \qquad (1)$$

can be adapted by translation b and dilatation a. By changing parameter a, we get a family of functions with different widths.

In this study, the so-called "Mexican hat" function (Fig. 1A, Combes et al. 1989) was adopted for the wavelet function $g(x)$, i.e. a time function of a modified gaussian type (the negative of the second derivative of Gauss function)

$$g(x) = (1 - x^2)e^{-x^2/2} \qquad (2)$$

This wavelet function has one of the best possible simultaneous concentration properties both in the time domain and in the frequency domain (Fig. 1B). The wavelet function of Eqn. (2) was applied to a flash-evoked impulse pattern of the retinal ganglion cell. For our purposes, the width of the wavelet function is 100 points (Fig. 1A). The width of wavelet function in the time domain (from 0.6 to 384 ms) is dependent on the time scale of the convoluted signal (Dirac pulses).

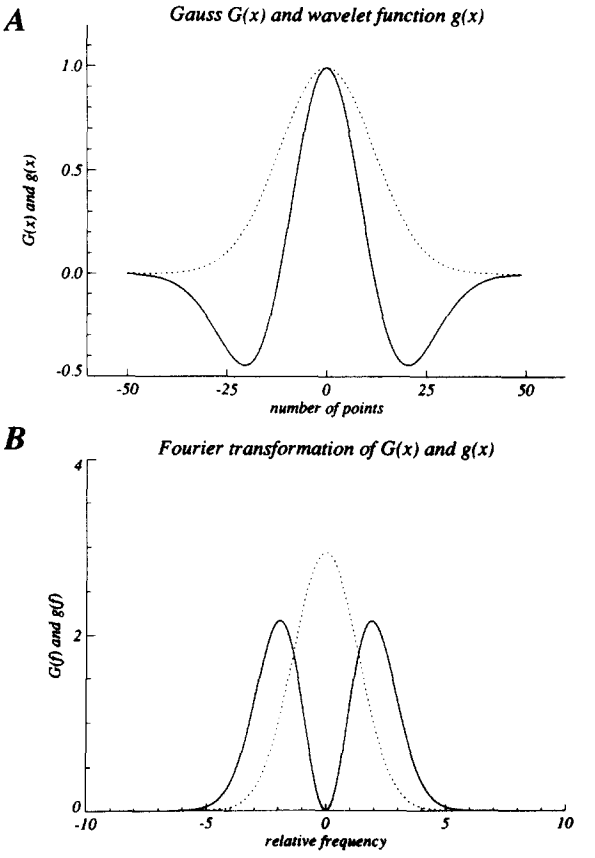

Fig. 1. A: Gauss function (dots) and wavelet function (Mexican hat, shown as a solid line) with which action potentials were convoluted; the duration of this function was varied from 0.6 to 384 ms for different steps of convolution. B: Fourier transformation of Gauss (dots) and wavelet function (solid line).

A wavelet function suitable for analysing nerve cell impulse trains should have the compatibility property, i.e. the integral of an individual wavelet equals 0 (Combes et al., 1989). In the following analysis the wavelet transformation (defined simply as wavelet in the illustrations) of a real signal $s(t)$ related to the wavelet function $g(x)$ under discussion is defined as the modified convolution:

$$W(b,a) = a^{-1/2} \int g\left(\frac{t-b}{a}\right) s(t)\, dt \qquad (3)$$

where $s(t)$ are Dirac pulses corresponding to the action potentials of analysed signals. We analysed

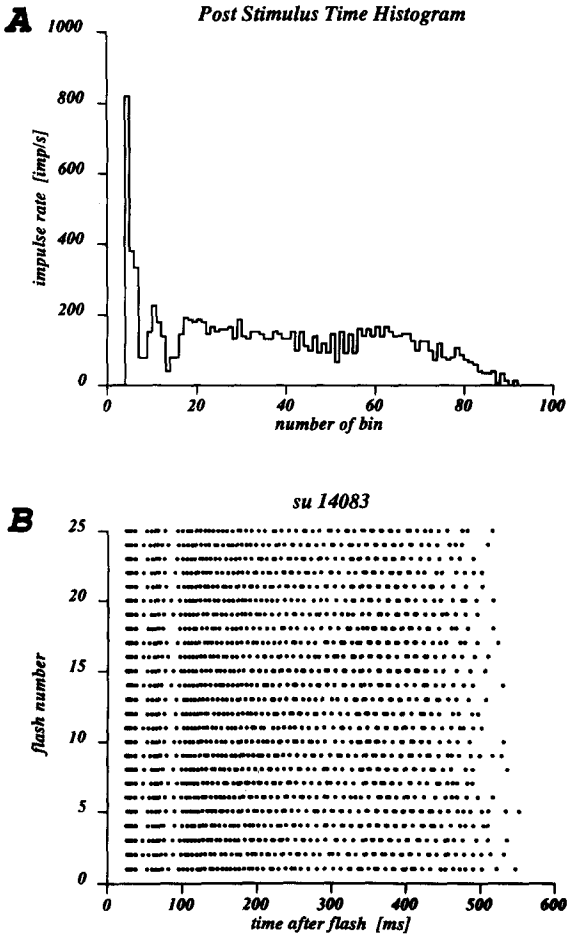

Fig. 2. A: post-stimulus time histogram (PSTH) of the on-center ganglion cell after twenty-five 10-ms light flashes, 100 bins, 6 ms bin duration. B: raster diagram for the same 25 flashes, same cell; time of analysis 600 ms.

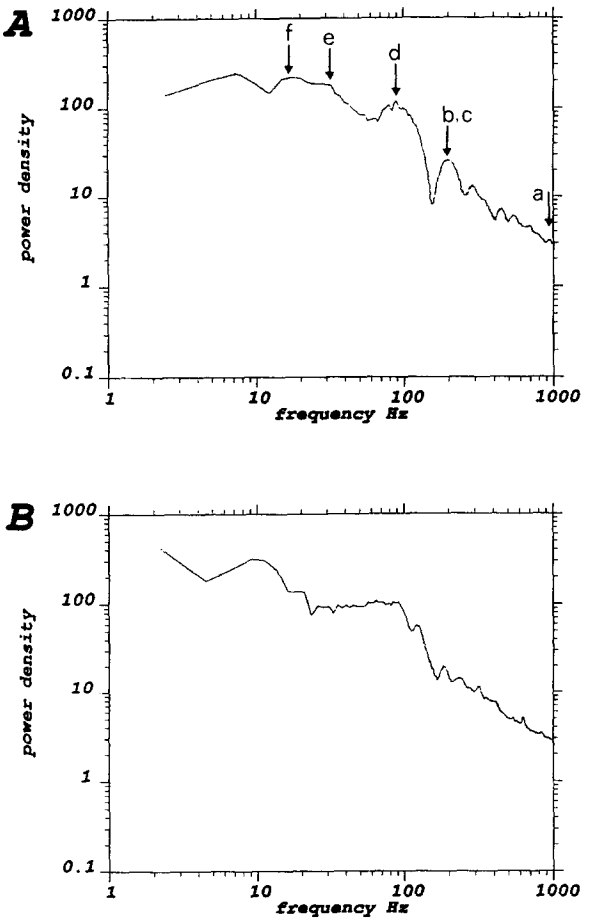

Fig. 3. Power spectra averaged 25 times from action potentials of on-center ganglion cell convoluted with function $\sin(x)/x$ after 10 ms light flashes with different intensities. A: 9.39 $cd \cdot m^{-2}$. B: 93.9 $cd \cdot m^{-2}$.

the responses of type-ON and type-OFF retinal ganglion cells to short flashes using wavelet transformation. We compared this method of analysis with that of PSTH and Fourier analysis of (a) a whole response convoluted with $\sin(x)/x$ function, and (b) part of a response convoluted with $\sin(x)/x$ function of appropriate frequency.

Results

Two examples of an analysis are given for the retinal ganglion cell flash response using wavelet transformation and PSTH. The first example is

that of the on-center ganglion cell. Fig. 2A is an example of a PSTH obtained from the flash responses of an on-center retinal ganglion cell of the cat retina (class I or Y-type; Grüsser et al., 1989). Fig. 2B is a corresponding raster diagram of the responses used to compute the PSTH. The oscillations which appear after flash do not necessarily appear in the PSTH. In Fig. 2A, the oscillations can be clearly seen between bin No. 40 and bin No. 60. The corresponding oscillations in Fig. 2B appear between 240 and 360 ms after flash (the intercepts are more spaced out). However, similar oscillations can also be seen between 360 ms and 500 ms. Whenever such oscillations are not locked to the flash, they are not visible in the PSTH regardless of binwidth. Fig. 3A illustrates the power density for the same data as in Fig. 2A and B. The arrows mark some of the local maxima of the power spectrum. By altering one parameter, i.e. the light flash intensity, these maxima do not appear for the same frequencies as demonstrated in Fig. 3B. The differences in their amplitudes are too small to be statistically significant after averaging 25 responses to the flashes. Fig. 4 is a "three-dimensional" picture of the wavelet transformation obtained when the widths of the wavelet function $g(x)$ (equation 2) were varied systematically in 20 steps from 6 to 120ms. This "three-dimensional" picture was transformed into an equivalent "two-dimensional" image (Fig. 5), whereas the amplitudes (z-axes of Fig. 4) were converted into different shades of grey; the higher the amplitude, the lighter the shading. Both figures present the same data, except that 640 were computed in Fig. 5 while 20 were computed in Fig. 4. The local maxima of the power spectrum demonstrated in Fig. 3 appear as oscillations in Fig. 5a–f. These oscillations were selected for closer examination and are depicted in Figs. 6 and 7. In each case, the left-hand graph represents the amplitude of wavelet transformation as a function of time; the right-hand graph represents the corresponding transformations in the frequency domain. In order to find transient oscillations in the spectra of neuronal responses, it is important to select the

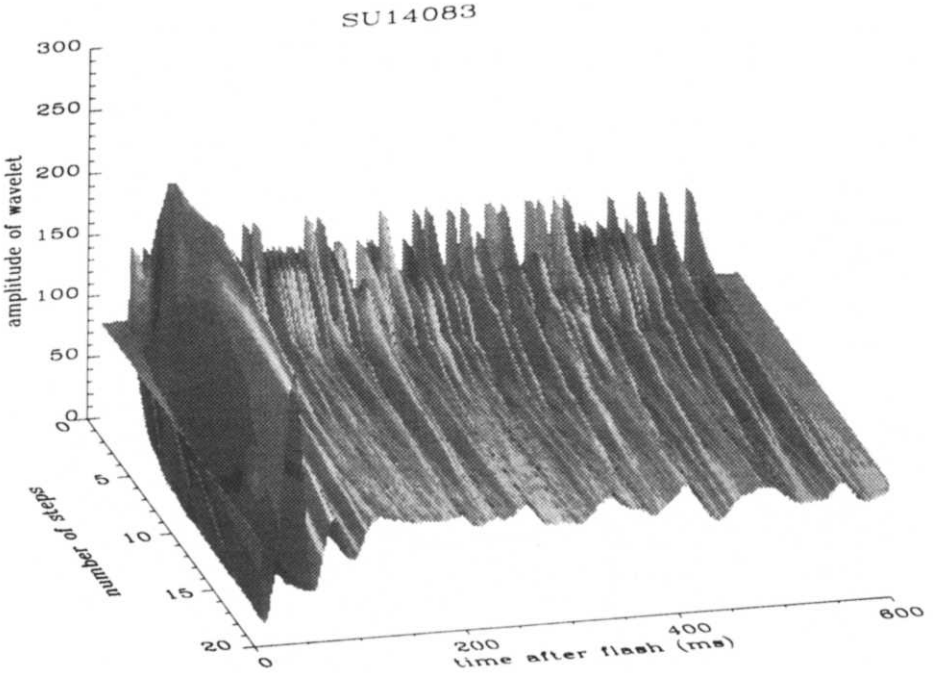

Fig. 4. 3D illustration of 20 steps (width of wavelet function increases by 6 ms with each step) of convolution of on-center ganglion cell discharges with Mexican hat function.

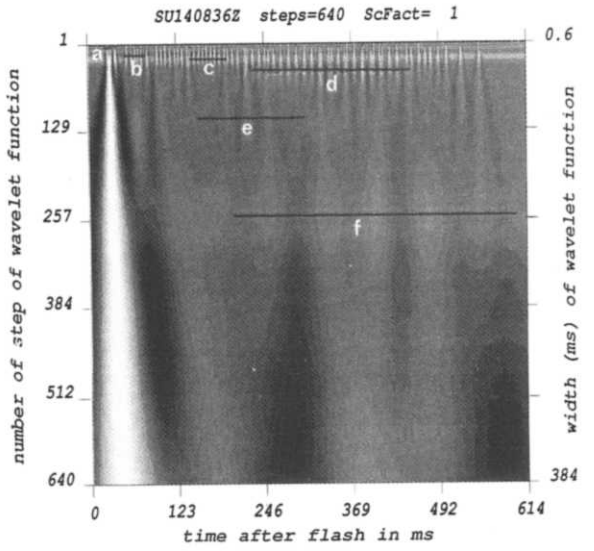

Fig. 5. Image picture of 640 steps of approximation of on-center ganglion cell response to light flashes (10 ms, 9.39 $cd \cdot m^{-2}$). The width of Mexican hat function was changed from 0.6 (top) to 384 ms (bottom). Black bars a–f denote are the occurrence of oscillations.

adequate wavelet function width. As can be seen in the raster diagram (Fig. 2B), the first fast oscillations appeared during the first impulse burst between 25 and 35 ms after the onset of the flash (Fig. 5a, and Fig. 6a). These oscillations, in the frequency range of 1000 Hz, represent the impact of the refractory period of the neuron cell. Another oscillation with a lower frequency occurs 50–80 ms after the flash (Fig. 5b, and Fig. 6b). A third appears 130–190 ms after the flash (Fig. 5c, and Fig. 6c). Beyond 150 ms after flash, transient oscillations with a lower frequencies were found (Fig. 5d–f, and Fig. 7d–f).

The difference in frequency of fast oscillations of ganglion cell responses to light flashes with various stimulus intensities (from 0.939 to 93.9 $cd \cdot m^{-2}$) was statistically analysed. The analysis was restricted to a time slot of about 10 ms, during which maximum impulse sequences were obtained (first peak in the PSTH of Fig. 2A). In order to find the oscillation frequencies in this initial slot, the power spectrum obtained by wavelet transformation was analysed using Hanning windows (Harris, 1978). The method for smoothing a power spectrum "smoothing over an ensemble of estimates" (Bendat and Piersol, 1971) was applied to reduce the random error. First the individual estimates from each of 10 successive responses were computed for independent sample responses by convoluting the impulse sequence with the wavelet function of equation (2). Then the individual estimates of each frequency in the power spectrum were averaged from the q data samples ($q = 10$). The resulting estimates are chi-square variables with 20 degrees of freedom, and normalized standard error of $\sqrt{0.1}$. The confidence range of power spectra computed by this method can be estimated in the following way:

Let us assume a 95% confidence interval (i.e. $1 - a = 0.95$) for a power spectrum density function $G(f)$ based upon an estimate $\hat{G}(f)$ (Bendat and Piersol, 1971):

$$\frac{2q\hat{G}(f)}{\chi^2_{2q;\alpha/2}} \leq G(f) < \frac{2q\hat{G}(f)}{\chi^2_{2q;1-\alpha/2}}$$

$$G(f) = 2 \lim_{T\to\infty} \frac{1}{T} E\{|X(f, T)|^2\}$$

where $X(f, T)$ is the finite Fourier transformation of a sample record x(t):

$$X(f, T) = \int_0^T x(t) e^{-j2\pi ft}\, dt$$

and the estimate of $G(f)$ is

$$\hat{G}(f) = \frac{2}{T} |X(f, T)|^2$$

with a resolution bandwidth $B = 1/T$, where T is the recorded length of a single sequence. Based on the 95% confidence interval for a power spectrum density function, the estimate was computed for the on-center ganglion cell and is shown in Fig. 8. It is clear that the fast oscillations of the early responses produce separate peaks. Furthermore, these peaks are significantly different for the three light intensities. In contrast, the peaks were hardly noticeable with a normal FFT procedure (Fig. 3A a–f) using the whole signal length, i.e. 800 ms from 20 ms after flash. This was particularly true for peak a and its corresponding peak in Fig. 3B.

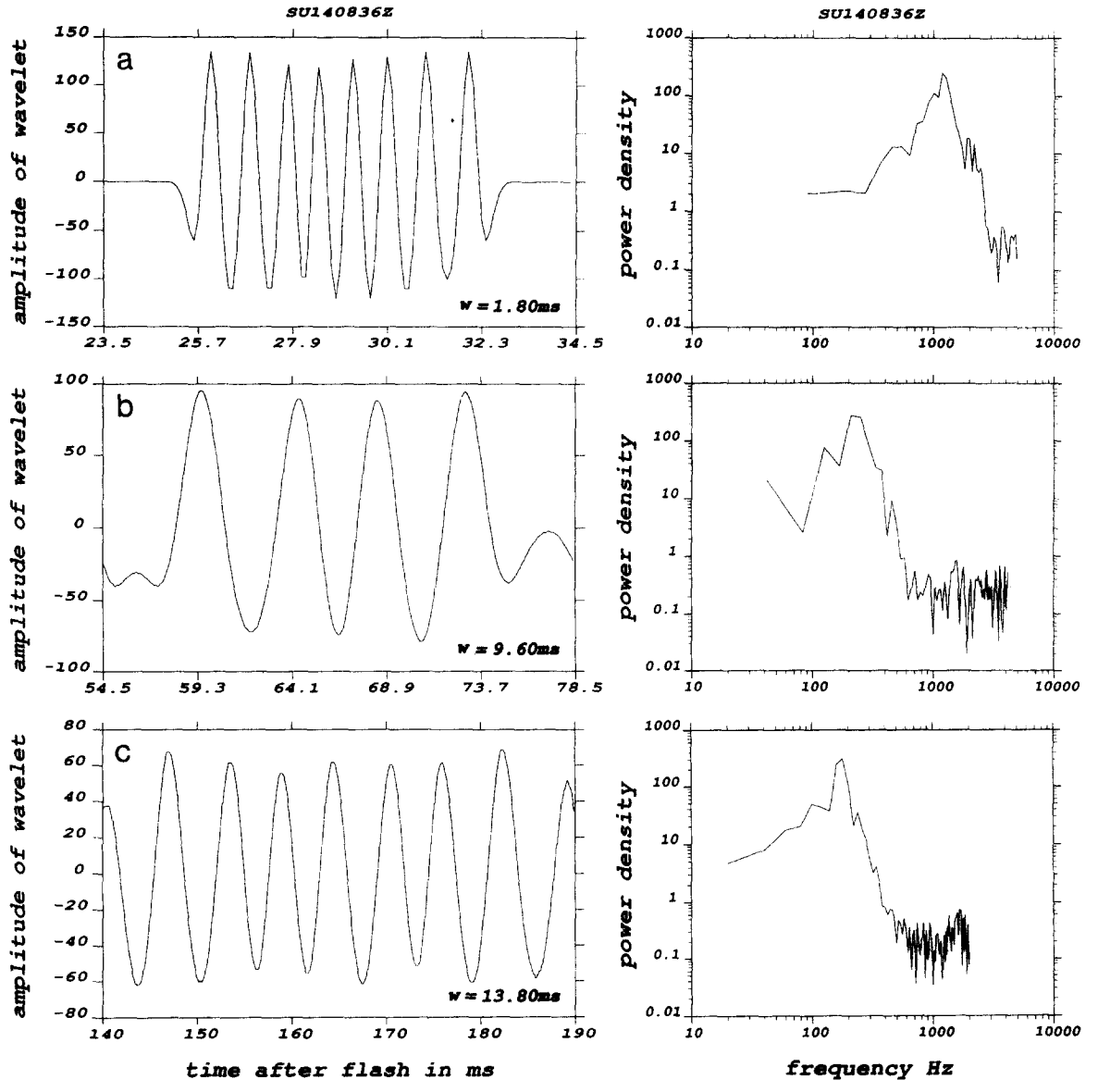

Fig. 6. Left: changes in amplitude of wavelet transformation for bars a, b, c in Fig. 5 rescaled and shown as a time function. "w = "denotes the width of the wavelet function. Right: Fourier analysis of the same signals with a Hanning window giving power spectrum density.

The second example of using the wavelet transformation is to apply it to off-center ganglion cell light flash responses and is shown in Fig. 9.

Fig. 9A depicts the PSTH averaged after 10 light flashes. An inhibition of ganglion cell activity lasting 200 ms after flash was followed by an excitation of activity of about 1000 ms, i.e. 200–1200 ms after flash.

After the initial inhibition, the light flash evoked an excitation in this ganglion cell followed by slow (about 5–6 Hz) oscillations (Fig. 9B, e; Fig. 9C, e). At the end of the excitation phase, oscillations with a frequency of about 10Hz ap-

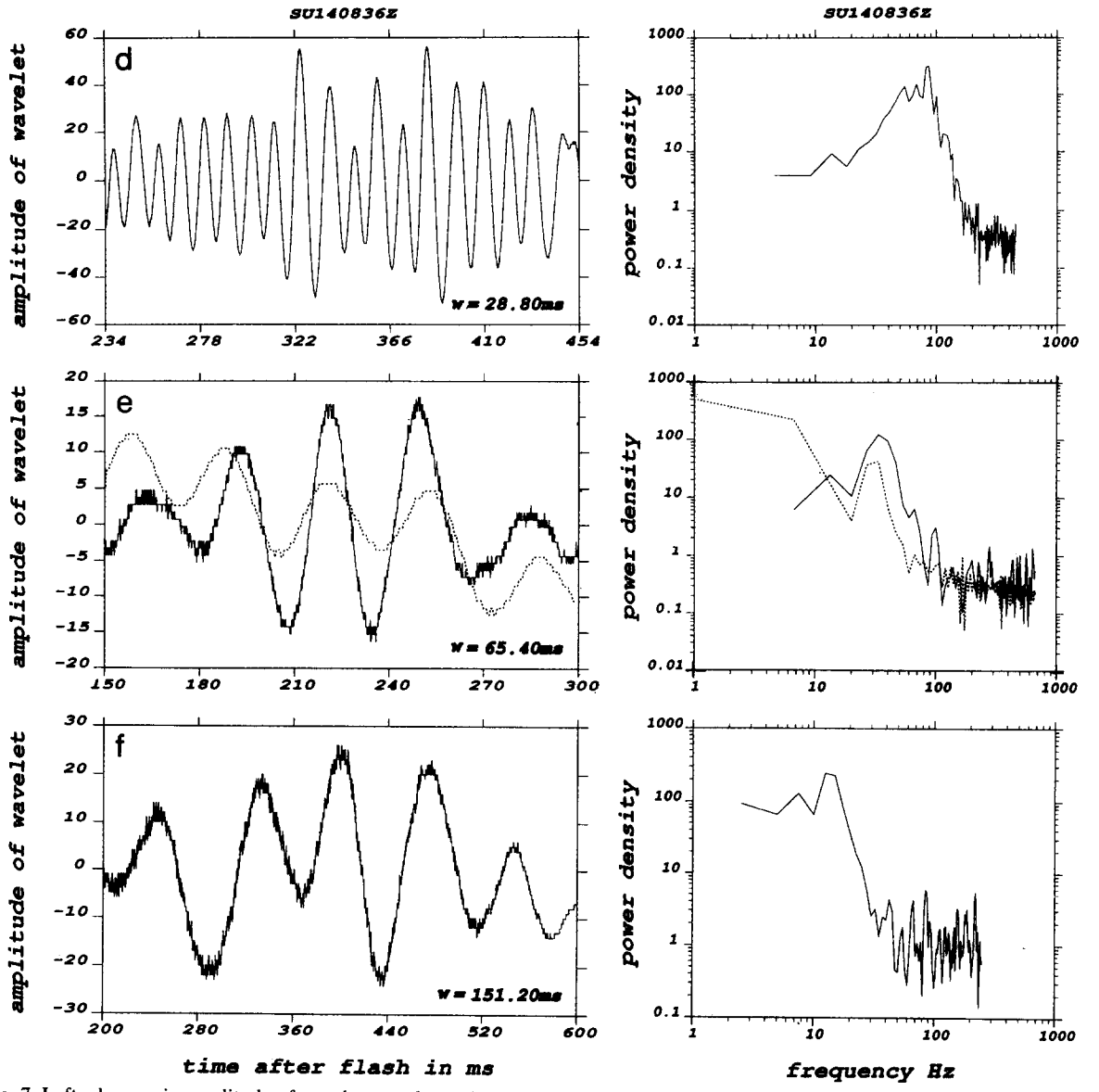

Fig. 7. Left: changes in amplitude of wavelet transformation for bars d, e, f in Fig. 5 rescaled and shown as a time function. "$w =$ " denoted the width of the wavelet function. Right: Fourier analysis of the same signals with a Hanning window giving power spectrum density.

peared (Fig. 9B, d, and Fig. 9C, d). An excitation phase of the off-center ganglion cell flash response was coded at two different frequencies of oscillations; fast oscillations with a frequency of about 130 Hz (Fig. 9B, a, and Fig. 9C, a), and others at about 30 Hz (Fig. 9B, b, and Fig. 9C, b). The second frequency also appeared later (Fig. 9B, c, and Fig. 9C, c).

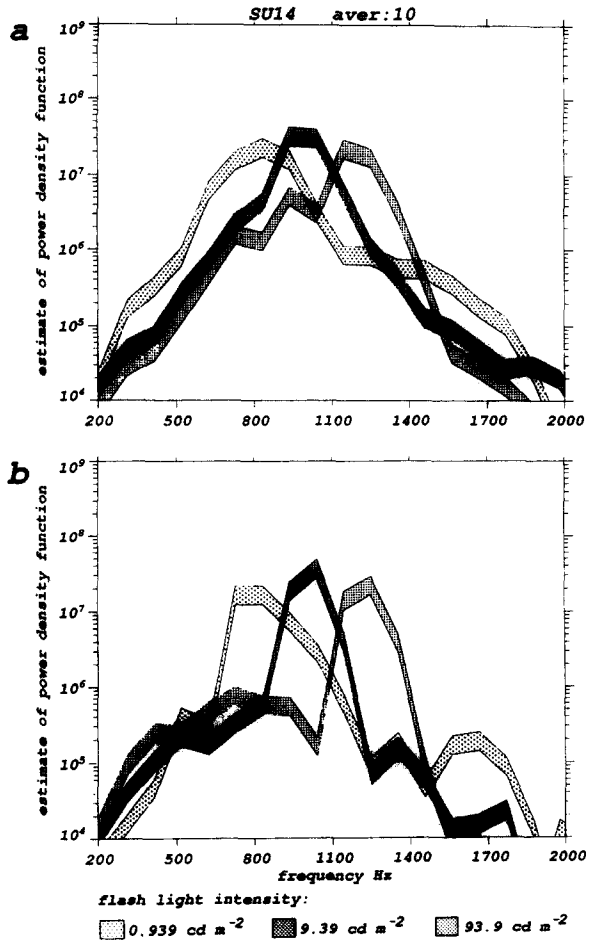

Fig. 8. Estimate of power density for the on-center ganglion cell class I as in Figs. 2–7, for 3 different light intensities. A: shaded areas denote increasing flash light intensity (95% confidence interval). Estimates were calculated with the same width of wavelet function; the window was fitted to the primary burst. B: estimates calculated from the difference between power density of action potential intervals in (A) and the power density of these same action potential intervals taken at random.

Discussion

In most of the responses of the CNS, the mean value of discharges measured in short intervals, for example PSTHs, changes strongly after stimulus (compare the PSTHs in Figs. 2A and 9A). This indicates that these signals are non-stationary so that their power spectral density or energy spectral density changes with time. The Fourier transformation does not preserve any time dependence and therefore cannot provide any information about changes in spectral characteristics. In the power spectra in Fig. 3, higher frequency components with short duration are represented by very small peaks compared with lower frequencies (compare peak a with peaks d and e in Fig. 3A). The wavelet transformation in Figs. 6 and 7 demonstrate that there are more periods of oscillations at higher frequencies (Fig. 6, a) than at lower frequencies (Fig. 7, d and e). This is not evident with the Fourier transformation in Fig. 3A, a, d, and e.

One of the best methods for analysing non-stationary signals (treated as quasi-stationary signals) in a short-time window is the spectrogram (Potter, Kopp and Green, 1947):

$$W_s(t, f) = \left| \int_{-\infty}^{\infty} s(u)h(t-u)e^{-j2\pi fu}\, du \right|^2$$

with $h(t)$ and $s(t)$ being a short-time window and a signal, respectively.

A similar method to the spectrogram is to pass the signal through a collection of bandpass filters and observe the output of each filter (a so-called sonogram; Potter et al., 1947). In both these methods, there is an unavoidable trade-off between frequency and time resolution. An increase in the frequency resolution through an increase in the window length decreases the time resolution. A short window results in a poor frequency resolution. This trade-off is circumvented in the wavelet transformation method by using different lengths of time windows and by choosing the appropriate width of wavelet function of each particular window (Fig. 5). It is difficult to find a suitable window for unknown non-stationary signals. This problem is solved by using the wavelet transformation method. The family of wavelet functions comprising different widths is convoluted with the signal and is intersected afterwards to find the best window (bars in Figs. 5 and 9A).

In order to extract the local oscillations in the signal, the wavelet function must have locality in the time and frequency domain.

One of the most used functions in electrophysiology is the $\sin(x)/x$ function (French and Holden, 1971). This function has the best concen-

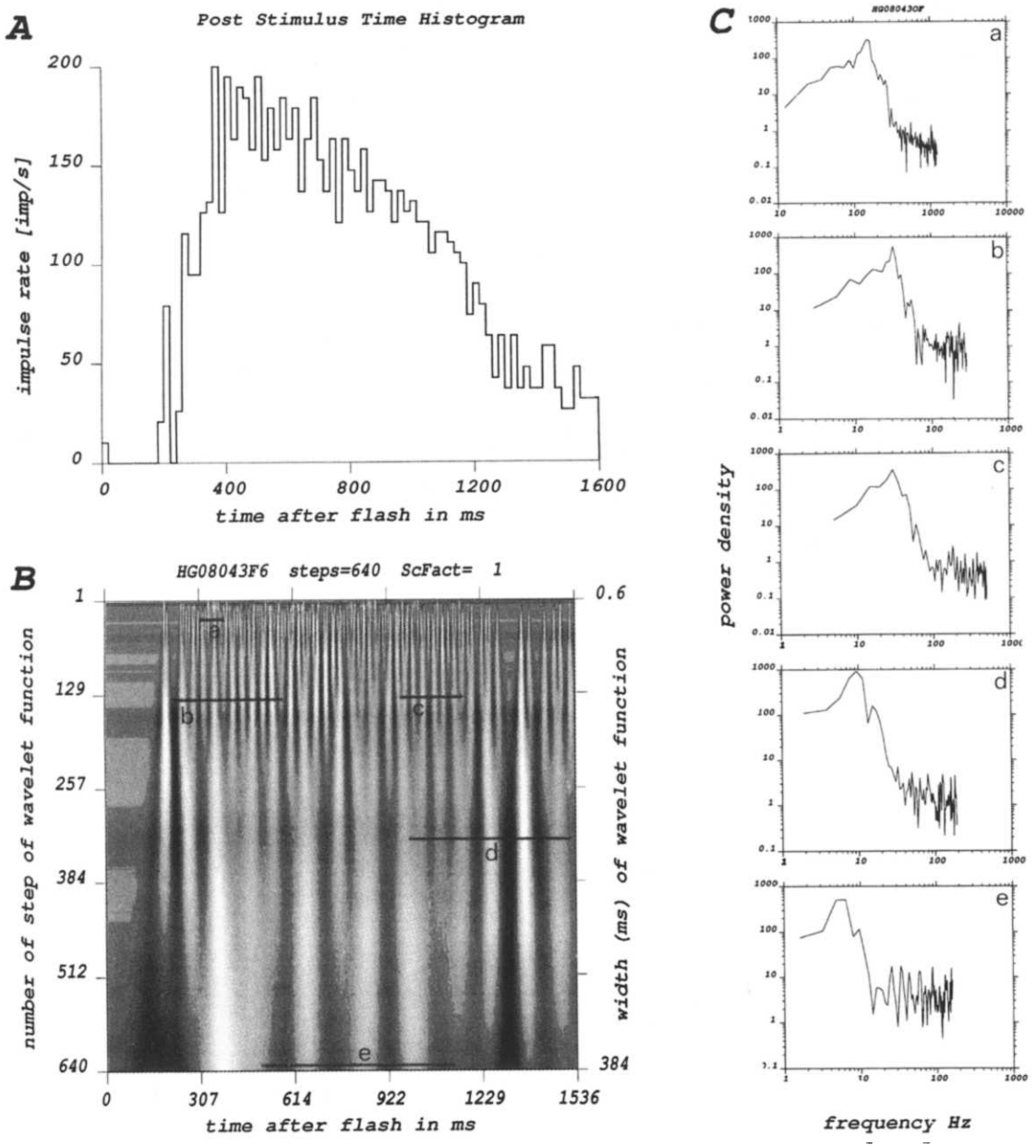

Fig. 9. A: post-stimulus time histogram (PSTH) of the off-center class I ganglion cell after ten 10-ms light flashes, 80 bins, 20 ms bin duration. Light intensity was 6.37 cd · m^{-2}. B: wavelet transformation for the same ganglion cell after the first flash (1536 ms). Transformation was performed with the Mexican hat function: wavelet function width from 0.6 to 394 ms. C: black bars in B a–e are transformed into a frequency domain and represented as power spectra density functions.

tration properties in the frequency domain but does not have locality in the time domain because its does not decrease fast enough in an exponential way. By substituting the wavelet function with the $\sin(x)/x$ function and its appropriate frequency, the oscillations extracted will be influenced by other parts of the signal. For example, in Fig. 7e, the dotted line was obtained from the

convolution of the signal using the $\sin(x)/x$ function; the solid line denotes the results obtained with the wavelet transformation. Both methods used the same time window (Fig. 5, e, for wavelet transformation). The influence the other parts of signal had on the oscillations using the $\sin(x)/x$ function (dotted line) resulted in an increase in the amplitude during the first and second period in comparison with the wavelet transformation. The $\sin(x)/x$ function also has no compatibility property which means that it is sensitive to the density of discharges; it is a low-pass filter whereas the wavelet functions are band-pass filters. Low frequency components are dominant for the $\sin(x)/x$ function (dotted line in Fig. 7e, right-hand power density graph). Mallat (1989) found it necessary to modify the $\sin(x)/x$ function in order to find orthonormal wavelets. These are used as conjugate quadrature filters for multiresolution analysis of the information contents of images.

In conclusion, our results suggest that wavelet transformation provides a comprehensive method for studying local transient oscillations in non-stationary signals from neuronal cells in the central nervous system.

Acknowledgements

The author would like to thank Prof. O.-J. Grüsser and Dr. B. Pöpel for their advice on the manuscript, Mrs. J. Dames and Miss C. Mahoney for their assistance with the English text, and Dipl. Ing. K-H. Dittberner for his help with the computations. Supported in part by a grant of DFG (grant 161).

Appendix

Comparison of the wavelet transformation with the Wigner distribution

An alternative approach to analysing non-stationary signals is to compute a function which approximates the instantaneous energy for a given time and frequency such as the Wigner distribution (Wigner, 1932; Classen and Mecklenbrauker, 1980):

$$W_s(t, f) = \int_{-\infty}^{\infty} s\left(t + \frac{\tau}{2}\right)\bar{s}\left(t - \frac{\tau}{2}\right)e^{-j2\pi f\tau}\,\mathrm{d}\tau$$

where $\bar{s}(t)$ is the complex conjugate of signal $s(t)$.

The Wigner distribution belongs to the Cohen class of functions which are bilinear shift-invariant in a time-frequency plane (Cohen, 1966). Classen and Mecklenbrauker (1980) demonstrated that any other distribution of the Cohen class may be considered as a spread version of the Wigner distribution, e.g. a spectrogram. The Rihaczek distribution (Rihaczek, 1968), which is also known as a coherent spectro-temporal intensity density function applied in auditory research (Eggermont et al., 1983), may also be considered as a spread version of the Wigner distribution. One of the shortcomings of the Wigner distribution is the interference phenomenon with the result that superposition of two signals causes oscillations or negative values to appear (Classen and Mecklenbrauker, 1980). In order to overcome this interference, smoothing or windowing of the transformed signal could be used. Smoothing, which is independent of time and frequency, leads to the smoothed pseudo-Wigner-Ville (Martin and Flandrin, 1985) or the pseudo-Wigner (Classen and Mecklenbrauker, 1980) distribution. However, it produces a spread in the frequency domain. The pseudo-Wigner distribution has been used to analyse human event-related potentials (Morgan and Gevins, 1986).

A second approach to the analysis of non-stationary signals is to find a class of functions which are invariant to shift and dilatation, the affine group, in the time domain (Flandrin, 1989). The "affine" distribution can be viewed as a generalization of the Wigner distribution for wideband signals and it has most of its properties (Flandrin, 1989). The wavelet transformation is an example of the "affine" distribution and could be interpreted as a way of modelling wideband signals, an example being the so-called sonar signals. Sonar signals represent natural signals emitted by bats or dolphins (Altes, 1976). These natural signals are first emitted and then received as dilated or

compressed signals which are shifted in time, functioning similarly to the wavelet transformation. The Fourier analysis of results obtained with the wavelet transformation is similar to constant-Q spectral analysis where changing scale parameters affects the bandwidth and the dominant frequency simultaneously. This means that the ratio bandwidth/dominant frequency is constant (Flandrin, 1989).

References

Altes, R.A. (1976) Sonar for generalized target description and its similarity to animal echolocation systems, J. Acoust Soc. Am., 59: 97–105.

Bendat, J.S. and Piersol, A.G. (1971) Random Data? Analysis and Measurement Procedures, Wiley–Interscience, New York, pp. 407.

Classen, T.A.C.M. and Mecklenbrauker, W.F.G. (1980) The Wigner distribution–a tool for time-frequency signal analysis, Phillips J. Res., 35: 217–250, 276–300, 372–389.

Cohen, L. (1966) Generalized phase-space distribution functions, J. Math. Phys., 7: 781–786.

Combes, J.M., Grossman, A. and Tchamitchian, Ph. (1989) Wavelets. Time-Frequency Methods and Phase Space, Springer-Verlag, Berlin, Heidelberg, New York, pp. 315.

Eggermont, J.J., Johannesma, P.I.M. and Aertsen, A.M.H.J. (1983) Reverse-correlation method in auditory research, Q. Rev. Biophys., 16: 341–414.

Flandrin, P. (1989) Some aspects of non-stationary signal processing with emphasis on time-frequency and time-scale methods. In J.M. Combes, A. Grossmann and P. Tchamitchian (Eds.), Wavelets, Time-Frequency Methods and Phase Space, Springer-Verlag, Berlin, Heidelberg, New York, pp. 68–98.

French, A.S. and Holden, A.V. (1971) Alias-free sampling of neuronal spike trains, Kybernetik, 8: 165–171.

Gabor, D. (1946) Theory of communications, J. IEE, 93: 429–457.

Grüsser, O.-J., Grüsser-Cornehls, U., Kusel, R. and Przybyszewski, A.W. (1989) Responses of retinal ganglion cells to eyeball deformation: a neurophysiological basis for "pressure phosphenes", Vis. Res., 29: 181–194.

Harris, F.J. (1978) On the use of windows for harmonic analysis with the discrete Fourier Transform. Proc. IEEE, 66: 51–83.

Mallat, S.G. (1989) A theory for multiresolution signal decomposition: the wavelet representation, IEEE Trans. Pattern Anal. Machine Intell., 11: 674–693.

Martin, W. and Flandrin, P. (1985) Wigner-Ville spectral analysis of non-stationary processes, IEEE Trans. Acoust. Speech Signal Process., ASSP-33: 1461–1470.

Morgan, N.H. and Gevins, A.S. (1986) Wigner distributions of human event-related brain potentials, IEEE Trans. Biomed. Eng., BME-33: 66–70.

O'Regan, R.G. and Przybyszewski, A.W. (1987) Power spectral analysis of chemoreceptor discharges during asphyxia and after administration of almitrine bismesylate. In J.A. Ribeiro and J. Pallot (Eds.), Chemoreceptors in Respiratory Control, Croom Helm, London, Sydney, pp. 342–350.

Potter, R.K., Kopp, G.A. and Green, H.C. (1947) Visible Speech, D. van Nostrand, Co., New York.

Rihaczek, A.W. (1968) Signal energy distribution in time and frequency, IEEE Trans. Inf. Theory, 14: 369–374.

Schild, D. and Schultens, H.A. (1986) The Fourier transform of a peristimulus time histogram can lead to erroneous results, Brain Res., 369: 353–355.

Wigner, E.P. (1932) On the quantum correction for thermodynamic equilibrium, Phys. Rev., 40: 749–759.